

overstrained thick-walled cylinder, limits the maximum level of the compressive residual bore stress beyond which the cylinder will yield in compression. Beyond the 2.0-diameter ratio then, it is anticipated that the slope of the autofrettaged curve will be the same as that for the nonautofrettaged condition.

The study of the fatigue characteristics of thick-walled cylinders directly, as in the manner described herein, has several experimental difficulties, the most significant being attrition of equipment. It would be desirable then to be able to predict the fatigue characteristics of thick-walled cylinders from some simplified fatigue test. One possible approach to this problem will now be discussed.

As the diameter ratio approaches 1, the radial component of the stress approaches 0 with only the tangential stress remaining. As shown in Fig. 16, the autofrettaged also approaches the nonautofrettaged condition as the diameter ratio decreases with convergence at $W = 1$. Since there is only one principal stress at the hypothetical case of $W = 1$, then it may be possible to correlate this condition with a uniaxial tensile-fatigue test. To a first approximation, the slopes of the diameter ratio versus cycles to failure curves for the nonautofrettaged condition are reasonably independent of stress level. Therefore, to determine the fatigue characteristics of thick-walled cylinders of a given material over a wide range of stress levels and diameter ratios would require only the running of a series of tensile-fatigue tests at different stress levels and to determine the slope, only one group of cylinders at a given diameter ratio and stress level. The slope of the diameter ratio versus cycles to failure curves is dependent upon cyclic-stress level for the autofrettaged condition. Consequently, two groups of thick-walled cylinders at widely different stress levels in conjunction with the tensile-fatigue data would be required to establish, to a close approximation, the entire family of curves for a wide range of diameter ratios and stress conditions of the type shown in Fig. 16 for the open-end condition, i.e., $\sigma_z = 0$. The feasibility of this simplified approach will be investigated further.

As the cyclic-stress level increases, the benefits from autofrettage decrease, and at stress levels approaching that for the overstrain pressure, there is little benefit. This is to be expected since the nonautofrettaged cylinders at these stress levels will actually permanently deform; thus, being autofrettaged to a certain degree on the first pressure cycle.

It should be noted that the least-squares lines shown in all of the figures intersect the ordinate which corresponds to 1000 cycles at a stress value closely approaching that for the 100 percent overstrain condition, i.e.,

$$\frac{\sigma_t - \sigma_r}{UTS} = \frac{1.08\sigma_y \ln W}{UTS} \left[\frac{2W^2}{W^2 - 1} \right] \quad (16)$$

where $1.08\sigma_y \ln W$ equals the pressure for 100 percent overstrain (3). If the least-squares line were continued to the one-cycle condition, the stress level would be well in excess of the rupture pressure which, for the material considered herein, is only slightly in excess of the overstrain pressure. Instead of continuing on, however, for the cyclic rates considered in this investigation, there is a leveling off in the very low cycle region and the slope of the curve approaches 0 at stress levels in the neighborhood of that associated with the 100 percent overstrain condition. This very low cycle, high stress region is a subject of current study.

Effect of Thermal Treatment After Autofrettage. It has been found in another current investigation that thermal treating high-strength autofrettaged cylinders at approximately 675 F for a period of time tends to increase the elastic load-carrying capacity. As shown in Fig. 17, thermal treatment, however, has little effect on fatigue characteristics as is indicated by the overlapping of the thermally and nonthermally treated data for autofrettaged cylinders in the 1.4 to 1.8-diameter ratio range. Except for this figure then, the thermally and nonthermally treated results were not considered separately.

Effect of Surface Finish and Tensile-Strength Variations. The internal diameter surface finishes of the specimens utilized in this program varied from approximately 16 to 125 RMS as measured along the longitudinal axis. However, analysis of the data does not indicate any trends toward dependency of the results upon surface finish over the range encountered.

The fatigue characteristics similarly appear to be proportional to the tensile-strength level for the range of ultimate tensile strength from 160,000 to 190,000 pounds per square inch.

Comparison of Results With Other Investigations. In Figs. 9, 10, 11, and 12, the data of other investigators, Morrison [1], and Newhall and Kosting [2], are included. In the case of the Newhall and Kosting data for large open-end cylinders at ultimate tensile-strength levels of 115,000 and 154,000 pounds per square inch, the correlation with the data presented herein is excellent. The Morrison data, however, for both the autofrettaged and nonautofrettaged condition, lies substantially above the presented data. In discussing this apparent discrepancy one must consider that there are three substantial differences in the experimental conditions between the two investigations. Whereas Morrison's specimens were tested as closed-end cylinders, the results presented herein considered the open-end condition, i.e., the longi-

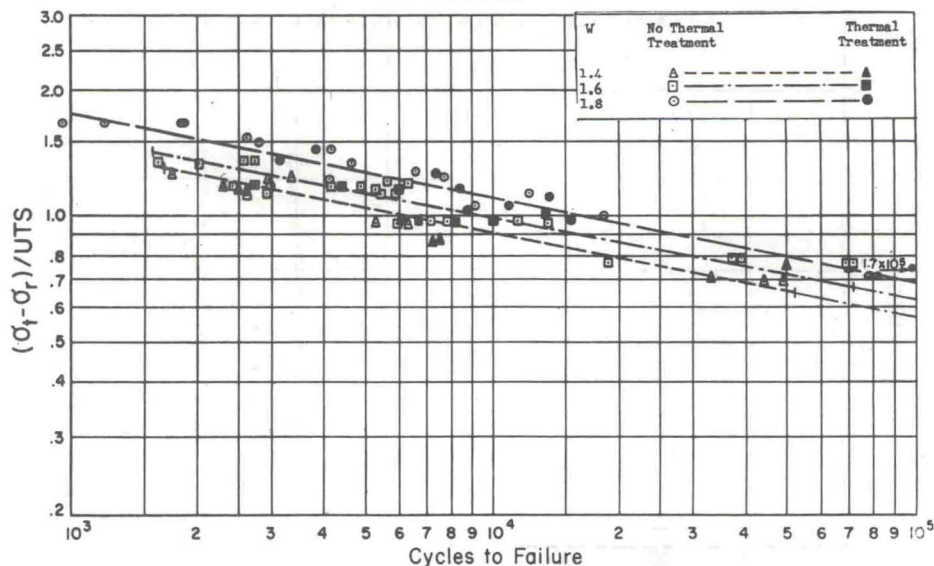


Fig. 17 Differences in principal bore stress versus cycles to failure for autofrettaged cylinders showing the effect of thermal treatment

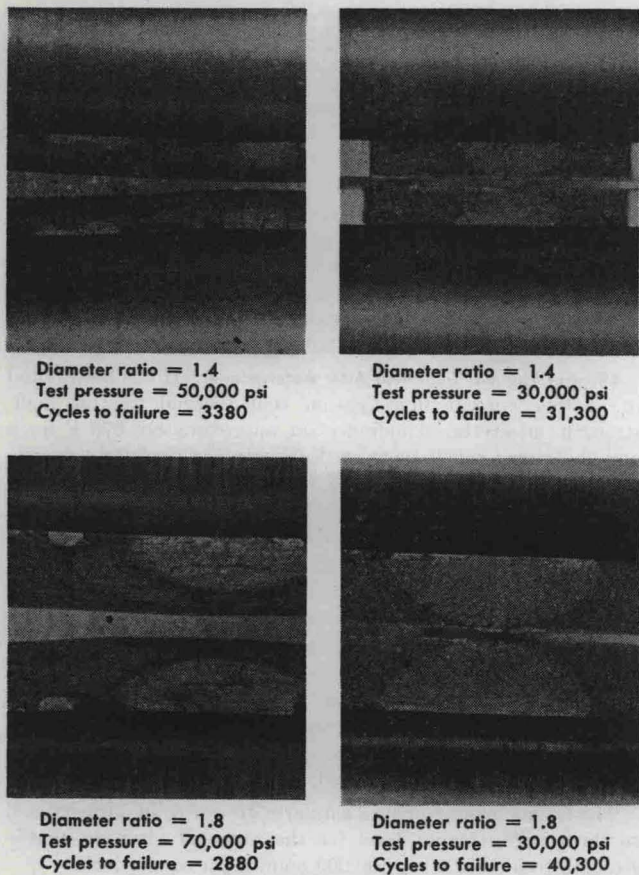


Fig. 18 Typical fatigue fractures

tudinal stress is effectively zero. If the third stress is taken into account theoretically by the octahedral stress parameter, equation (9), the variation is slightly reduced. Except by test, one cannot be certain of the magnitude of the effect of this third stress on fatigue. Therefore, the magnitude by which the third principal stress associated with the closed-end condition affects fatigue is the subject of a current investigation. Second, Morrison used a cyclic pressure rate of approximately 1000 cycles per minute as compared to 6 per minute for this investigation.

Third, the bore of Morrison's specimens were lapped to a finish of approximately 1 to 4 RMS as compared to 16 to 125 RMS which could have a pronounced effect in terms of crack initiation. It is difficult to ascertain the magnitude of the contribution of these various differences to the higher fatigue characteristics reported by Morrison. It is most likely, however, that the most important factor is the difference in surface finish. It is interesting to note that the discrepancy is substantially smaller in the case of the autofrettaged data as compared to the nonautofrettaged condition. This is probably due in part to the tendency for the high compressive tangential residual stress to reduce the effectiveness of the rougher bore surface in enhancing crack initiation.

Fracture Analysis. Representative fatigue failures for thick-walled cylinders of 1.4 and 1.8-diameter ratio at low-cyclic and high-cyclic stress levels are shown in Fig. 18. As can be noted, there are two characteristic zones. The first zone, which appears lighter, has a smooth appearance with conchoidal markings. This zone, sometimes called the zone of decohesion [6], is characteristic of a cyclically propagating fatigue crack. The second and remaining zone has a fibrous texture which is characteristic of static rupture in a ductile thick-walled cylinder.

From a macroscopic standpoint, the fatigue crack evidently propagates to the depth at which the remaining material is no longer able to withstand the internal pressure, and ductile rupture occurs. As would be expected then, there should be a correlation between the cyclic stress and the fatigue fracture area and depth. By examining a large number of fracture surfaces of the specimens associated with this study, it has been found that there is an approximate linear relationship between the cyclic-stress parameter and the crack depth divided by the wall thickness as shown in Fig. 19. There is, of course, scatter due to the experimental difficulty of determining the exact location of the boundary between the fatigue crack and fibrous rupture zone, as well as the statistical nature of fatigue data. However, the scatter is not so great that the linear correlation cannot be readily detected over a wide range of cyclic-stress levels and wall ratios. A similar linear relationship also exists for the cyclic-stress parameter versus the crack area divided by the square of the wall thickness.

It should be noted that only the fatigue crack causing final failure was considered in the above plots. Smaller cracks were also noted in several other areas of the specimen. An example of this condition is shown in Fig. 18, where several smaller fatigue cracks are readily visible.

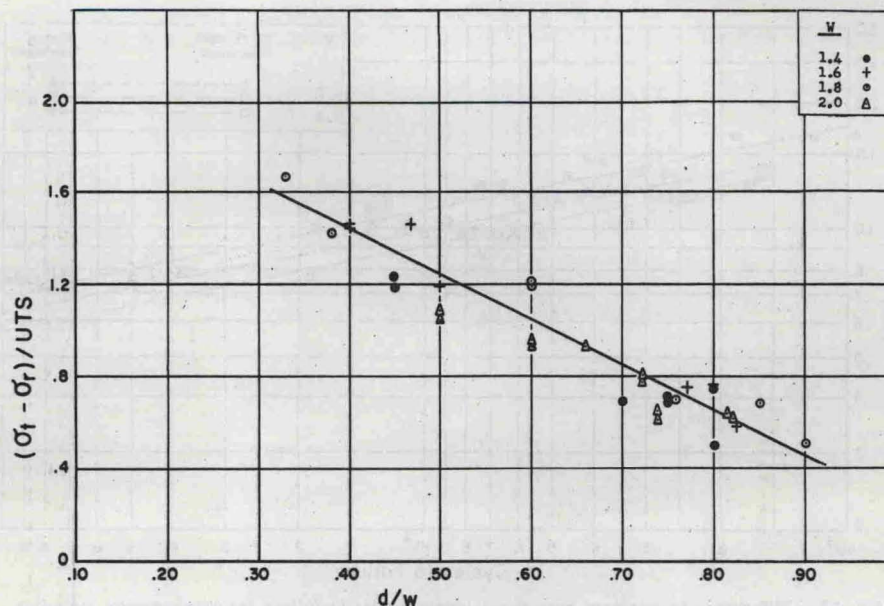


Fig. 19 Difference in principal bore stress versus crack depth/thickness